



# Gravitational Wave Astronomy: Detection Methods and Astrophysical Implications

Sini R

*Assistant Professor, Department Of Physics, Providence Women's College (Autonomous), Calicut, Kerala, India*

## Kerala Article Information

Received: 5<sup>th</sup> February 2026

Received in revised form: 7<sup>th</sup> March 2026

Accepted: 8<sup>th</sup> April 2026

Available online: 14<sup>th</sup> May 2026

Volume: 2

Issue: 2

DOI: <https://doi.org/10.5281/zenodo.20151550>

## Abstract

The direct detection of gravitational waves in September 2015 by the Advanced LIGO observatories opened a new observational window on the universe. In less than a decade the field has transitioned from a single detection to a catalogue of nearly a hundred compact-binary coalescences, together with the multi-messenger observation of a binary neutron-star merger in 2017 that simultaneously produced gravitational waves, electromagnetic emission, and kilonova signatures. This paper reviews the theoretical background of gravitational waves, the principles and performance of laser-interferometric detectors, the catalogue of significant detections, and the astrophysical implications for compact-object populations, tests of general relativity, cosmology, and the origin of heavy elements. Future detector generations LIGO Voyager, the Einstein Telescope, Cosmic Explorer, and the space-based LISA are expected to extend reach to high redshifts and to lower frequencies inaccessible to ground-based instruments.

**Keywords:** Gravitational Waves, LIGO, Multi-Messenger Astronomy, Compact Binary Coalescence, General Relativity, LISA.

## 1. INTRODUCTION

Gravitational waves were predicted by Einstein in 1916 as a consequence of the linearised field equations of general relativity.<sup>3</sup> In the weak-field limit the Einstein equations reduce to a wave equation propagating at the speed of light, with two polarisation modes traditionally labelled 'plus' and 'cross', corresponding to quadrupolar distortions of test-mass separations transverse to the propagation direction. For decades following Einstein's prediction, the physical reality of gravitational waves was disputed: even Einstein himself briefly believed in 1936 that the waves were coordinate artefacts, a view later reversed following theoretical work by Bondi, Pirani, and Feynman establishing their physical existence through the concept of energy transport by gravitational radiation.<sup>1</sup> The 'sticky bead' argument of Feynman and the Bondi news-function analysis established that gravitational waves must carry energy away from their sources and can perform work on matter.

The indirect evidence for gravitational-wave emission was provided by the Hulse Taylor binary pulsar PSR B1913+16, discovered in 1974. Continuous timing of this system over four decades revealed orbital decay consistent with general-relativistic emission of gravitational radiation to better than one per cent precision, earning Hulse and Taylor the 1993 Nobel Prize in Physics.<sup>4</sup> Subsequent binary-pulsar systems notably the double pulsar PSR J0737–3039 have extended these tests of the quadrupole formula and confirmed additional post-Newtonian effects. Nevertheless, direct detection of gravitational waves remained elusive because the intrinsic weakness of the gravitational interaction translates into strain amplitudes of order  $10^{-21}$  at Earth from astrophysical sources, requiring kilometre-scale laser interferometers to resolve.

The first direct detection, GW150914, was announced in February 2016 following joint observation by the two LIGO detectors at Hanford and Livingston on 14 September 2015, during the first engineering run of the Advanced LIGO detectors.<sup>1</sup> GW150914 corresponded to the merger of two stellar-mass black holes of approximately 36 and 29 solar masses at a luminosity distance of approximately 410 Mpc (redshift  $z \approx 0.09$ ); the coalescence produced a final 62-solar-mass black hole with three solar masses of energy radiated as gravitational waves, corresponding to a peak luminosity briefly exceeding the combined electromagnetic output of all stars in the observable universe. The discovery earned Weiss, Barish, and Thorne the 2017 Nobel Prize in Physics. In August 2017, the GW170817 binary neutron-star merger was observed in coincidence with a short gamma-ray burst (GRB 170817A) detected by Fermi GBM 1.7 s after the merger, and subsequent electromagnetic follow-up across radio, optical, X-ray, and ultraviolet bands identified the kilonova AT2017gfo in the galaxy NGC 4993, inaugurating multi-messenger gravitational-wave astronomy.<sup>2</sup> Spectroscopic analysis of the kilonova provided direct observational evidence for r-process nucleosynthesis of heavy elements, including gold, platinum and lanthanides, in compact-object mergers.

## 2. THEORETICAL BACKGROUND

In the weak-field limit the metric may be written as:

$$g_{\mu\nu} = \eta_{\mu\nu} + h_{\mu\nu} \text{ with } |h_{\mu\nu}| \ll 1 \quad (1)$$

where  $\eta_{\mu\nu}$  is the Minkowski metric and  $h_{\mu\nu}$  a small perturbation. Imposing the Lorenz gauge  $\partial_\mu \bar{h}^{\mu\nu} = 0$  on the trace-reversed perturbation:

$$\bar{h}_{\mu\nu} \equiv h_{\mu\nu} - \frac{1}{2}\eta_{\mu\nu}h \quad (2)$$

reduces the Einstein field equations to:

$$\square \bar{h}_{\mu\nu} = -\frac{16\pi G}{c^4} T_{\mu\nu} \quad (3)$$

which in vacuum becomes a simple wave equation with solutions propagating at the speed of light.<sup>3</sup> The transverse-traceless (TT) gauge further restricts  $h_{\mu\nu}$  to its physical two-polarisation content, explicitly exhibiting the quadrupolar 'plus' and 'cross' polarisation modes. Emission is governed by the quadrupole formula: the luminosity:

$$L = \frac{G}{5c^5} \langle \ddot{Q}_{ij} \ddot{Q}^{ij} \rangle \quad (4)$$

where  $Q_{ij}$  is the mass-quadrupole moment and the triple dot denotes the third time derivative. For a binary of chirp mass:

$$M_{\text{chirp}} = \frac{(m_1 m_2)^{3/5}}{(m_1 + m_2)^{1/5}} \quad (5)$$

the strain amplitude scales as:

$$h \propto \frac{\left(\frac{GM_C}{c^2}\right)^{5/3} \left(\frac{\pi f}{c}\right)^{2/3}}{D} \quad (6)$$

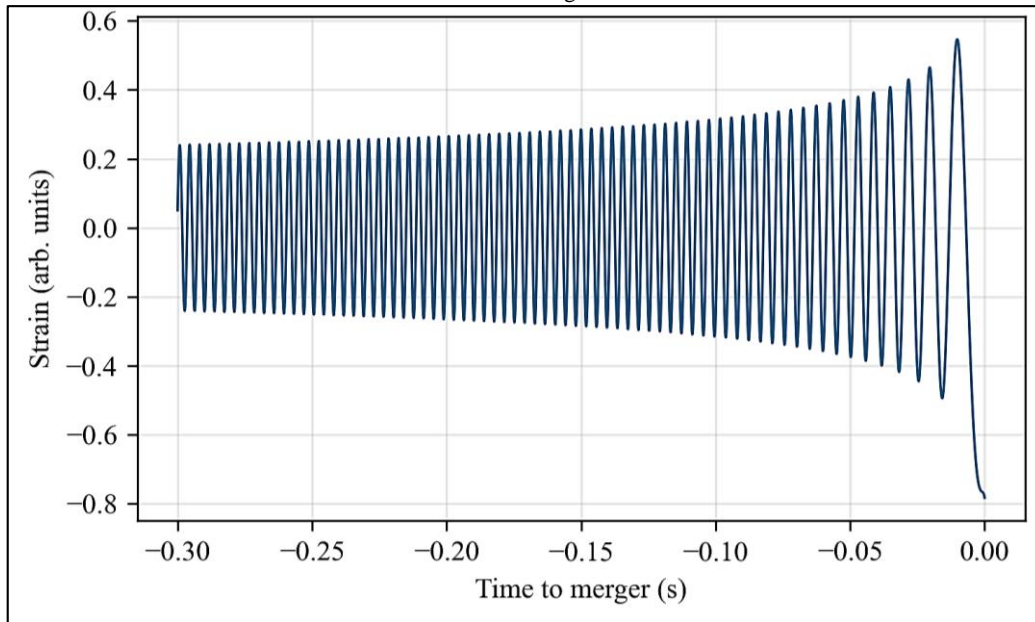
and the frequency evolves as:

$$\frac{df}{dt} \propto f^{11/3} \quad (7)$$

producing the characteristic chirp waveform (Figure 1). This phase evolution provides the principal observable for measuring the chirp mass, which is the best-constrained source parameter in compact-binary detections. Post-Newtonian expansions systematically include higher-order corrections in  $v/c$ ; effective-one-body formalisms resum the post-Newtonian series into a one-body problem with modified Hamiltonian; and numerical-relativity simulations solve the full Einstein equations during merger. Together these techniques provide template banks used for matched-filter searches<sup>5</sup>. Inspiral, merger, and ringdown are modelled respectively by post-Newtonian expansions, full numerical relativity, and black-hole perturbation theory with quasi-normal modes; modern phenomenological and surrogate waveform families (IMRPhenom, SEOBNR, NRSur) integrate these regimes.

Direct detection is possible because the strain signal, though minute, is coherent and has a well-modelled waveform. Matched filtering cross-correlates the detector output with template waveforms parameterised by source physics; the signal-to-noise ratio accumulates coherently over the many cycles of the inspiral, allowing detection of signals whose peak strain lies well below the instantaneous noise floor. Interferometric detectors compare the round-trip light-travel times along two orthogonal arms; a passing gravitational wave alternately lengthens one arm while shortening the other, producing a phase shift at the photodetector that scales linearly with the strain amplitude. Because the detectors measure strain rather than energy, sensitivity degrades only as the luminosity distance (rather than the inverse-square law), giving gravitational-wave astronomy disproportionate reach compared with electromagnetic surveys of comparable aperture.

Fig 1: Illustrative chirp waveform for a compact-binary coalescence. Frequency and amplitude increase until merger.<sup>1,5</sup>



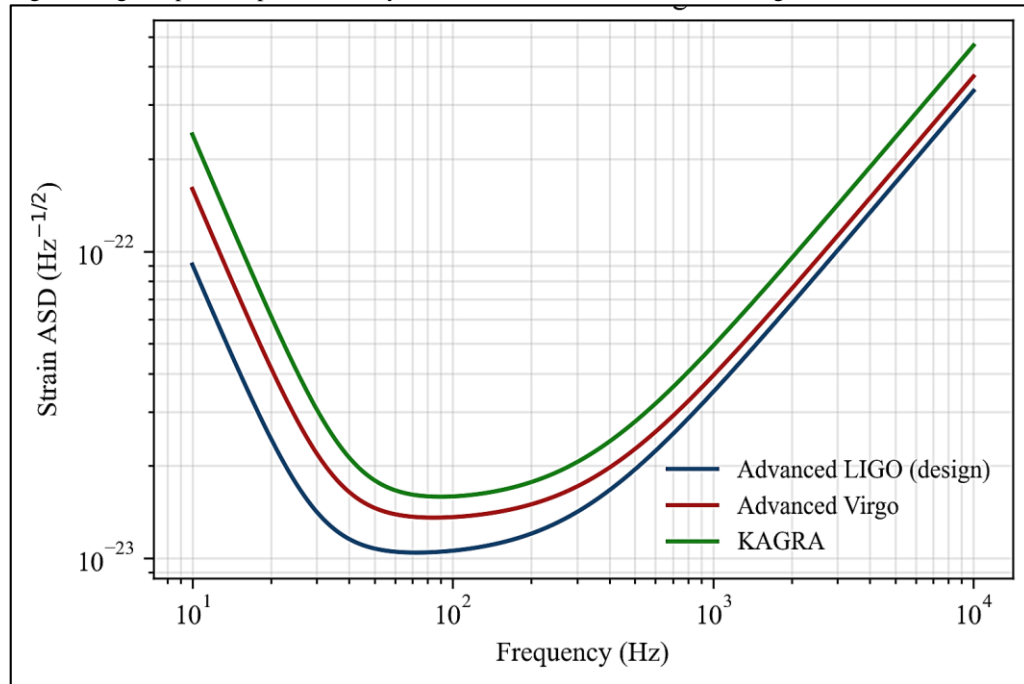
### 3. DETECTION METHODOLOGIES

The Advanced LIGO detectors use 4 km Fabry-Perot-enhanced Michelson interferometers with power and signal recycling, operating near quantum noise limits in the 100–1000 Hz band. Laser power of 100–200 kW circulates in each arm cavity (amplified from a 200 W input via power recycling), increasing the photon flux and consequently reducing shot noise. Signal recycling further tunes the frequency response. Test masses are 40 kg fused-silica mirrors suspended as quadruple pendulums providing seismic isolation in the detection band. Advanced Virgo (3 km arm length) in Italy and KAGRA (underground cryogenic, 3 km arm length, sapphire test masses cooled to 20 K) in Japan now operate as part of the international network.<sup>1,6</sup>

The design sensitivities are shown in Figure 2. At different frequencies distinct noise sources dominate: below 10 Hz the detectors are limited by seismic noise, residual mirror motion transmitted through the suspension chain, and Newtonian (gravity-gradient) noise from atmospheric and terrestrial mass movements that couple gravitationally to the test masses and cannot be shielded. Between 10 and 50 Hz, thermal noise in the test-mass coatings and in the suspension wires dominates; minimising thermal noise motivates cryogenic operation (implemented in KAGRA) and the development of crystalline or low-loss coating materials. Above ~100 Hz, quantum shot noise of the laser dominates; squeezed-light injection, in which vacuum fluctuations are 'squeezed' to redistribute uncertainty between conjugate variables, has been used to further reduce shot noise in the high-frequency band. Both LIGO and Virgo have operated with frequency-dependent squeezing since 2019, achieving 3–6 dB noise reduction in parts of the detection band.<sup>7</sup> Frequency-dependent squeezed-light filtering via a long filter cavity allows sensitivity improvement across the full detection band without sacrificing low-frequency performance.

Signal identification relies on matched-filter search pipelines that cross-correlate detector strain data against template banks of expected waveforms, typically containing  $10^5$  to  $10^6$  templates covering the astrophysically relevant parameter space in mass and spin. Coincident triggers across multiple detectors within light-travel-time windows establish candidate events, with background distributions estimated by time-sliding data streams to suppress accidental coincidences. Parameter estimation uses Bayesian inference with Markov-chain Monte Carlo or nested sampling to reconstruct the posterior distribution over source parameters (masses, spins, sky position, distance, inclination, polarisation). Low-latency pipelines such as GstLAL, MBTA, and PyCBC Live provide alerts to astronomical facilities within minutes to support electromagnetic follow-up, while offline deep analyses refine significance estimates and parameter measurements.

Fig 2: Design amplitude spectral density of the Advanced LIGO, Advanced Virgo and KAGRA detectors.<sup>6,7</sup>



#### 4. CATALOGUE OF EVENTS

The first three LIGO–Virgo observing runs produced the Gravitational-Wave Transient Catalogues GWTC-1 (first observing run, O1), GWTC-2 (O2 and first half of O3), and GWTC-3 (full O3), comprising approximately 90 significant compact-binary coalescence candidates.<sup>8</sup> The catalogue is dominated by binary black-hole (BBH) mergers with component masses ranging from approximately 5 to 85 solar masses. The BBH mass distribution exhibits rich structure: a primary peak near 35 solar masses consistent with the pulsational pair-instability mass gap, a secondary peak near 10 solar masses possibly reflecting compact-binary formation channels, and a rising tail toward low masses.

Several events merit specific mention. GW150914, the first detection, remains the most spectacular BBH event: two black holes of 36 and 29 solar masses coalescing at 410 Mpc produced a signal with signal-to-noise ratio of 24 and established the template for subsequent discoveries. GW170817, the first binary neutron-star (BNS) merger, detected on 17 August 2017, enabled the first multi-messenger gravitational-wave observation, with electromagnetic counterparts across radio through X-ray bands. The kilonova AT2017gfo provided the first direct spectroscopic evidence of r-process nucleosynthesis of heavy elements in compact-object mergers. GW170817 also provided the first measurement of the speed of gravitational waves to within  $10^{-15}$  of  $c$ , and constrained the neutron-star equation of state through the tidal deformability parameter  $\tilde{\Lambda}$ .

GW190521, detected on 21 May 2019, is arguably the most surprising single event: a merger with progenitor masses 85 and 66 solar masses, producing a 142-solar-mass remnant. The primary mass fell within the pulsational pair-instability mass gap of 65–120 solar masses, suggesting dynamical formation possibly including a previous merger product rather than the isolated-binary evolution channel typical of lighter BBHs. GW190425 (April 2019) was the second BNS detection; GW190412 was a strongly asymmetric BBH with mass ratio near 0.3; and GW200115/GW200105 in early 2020 provided the first confident neutron-star black-hole (NSBH) detections. Binary neutron-star and neutron-star black hole systems provide additional benchmarks for constraining the nuclear equation of state and the physics of compact-object formation (Table 1).

Table 1. Selected milestone gravitational-wave events and their key parameters.<sup>1,2,8</sup>

Event	Date (UT)	Source type	Primary / secondary ( $M_{\odot}$ )	Luminosity distance (Mpc)
GW150914	14-Sep-2015	BBH	36 / 29	410
GW151226	26-Dec-2015	BBH	14 / 8	440
GW170817	17-Aug-2017	BNS	1.48 / 1.26	40
GW170814	14-Aug-2017	BBH (3-detector)	30 / 25	540
GW190521	21-May-2019	BBH (upper mass gap)	85 / 66	5300
GW200115	15-Jan-2020	NSBH	5.7 / 1.5	300

## 5. ASTROPHYSICAL IMPLICATIONS

Gravitational-wave observations have delivered four categories of scientific return. First, they characterise the population of stellar-mass compact objects: mass functions, spin distributions, and formation-channel indicators now constrain isolated-binary evolution versus dynamical-formation scenarios<sup>9</sup>. The black-hole mass distribution extracted from GWTC-3 shows structure including a peak near 35 solar masses plausibly associated with the pulsational pair-instability boundary, a secondary feature near 10 solar masses, and a rising power-law tail at low masses. Spin distributions suggest a significant fraction of sources with low aligned spins, consistent with isolated-binary channels, together with a minority of high-spin or misaligned-spin systems suggestive of dynamical formation in dense stellar environments. Merger-rate densities are approximately 20–40 Gpc<sup>-3</sup> yr<sup>-1</sup> for binary black holes, 10–1700 Gpc<sup>-3</sup> yr<sup>-1</sup> for binary neutron stars, and 8–140 Gpc<sup>-3</sup> yr<sup>-1</sup> for neutron-star–black-hole systems.

Second, gravitational-wave observations test general relativity in the strong-field regime. Constraints include: propagation speed  $v_g=c$  to  $10^{-15}$  from GW170817/GRB 170817A coincidence), dispersion, graviton mass  $m_g < 10^{-23}$  eV/c<sup>2</sup>, parameterised post-Newtonian deviations, black-hole ringdown spectroscopy (quasi-normal modes consistent with Kerr), and tests of the no-hair theorem via multiple-mode ringdown analyses.<sup>10</sup> No statistically significant deviations from general relativity have been observed in any regime probed to date, substantially constraining modified-gravity alternatives.

Third, GW170817 enabled r-process nucleosynthesis measurements through kilonova spectroscopy, confirming compact mergers as principal sources of elements heavier than iron.<sup>2</sup> Infrared spectral features at 0.8 and 2.1 microns in AT2017gfo have been attributed to strontium and possibly other heavy lanthanide-region elements, providing the first direct evidence of r-process nucleosynthesis in a single astrophysical event. Total ejected r-process material of order 0.05 solar masses per event is consistent with binary neutron-star mergers contributing a substantial fraction of galactic heavy elements.

Fourth, standard-siren cosmology measurements exploit the fact that gravitational-wave sources directly encode their luminosity distance, with no reliance on the conventional cosmological distance ladder. Combining a gravitational-wave distance measurement with an electromagnetic redshift (for multi-messenger events like GW170817) or with galaxy-catalogue information (for 'dark sirens') yields independent Hubble-constant measurements.<sup>11</sup> The present uncertainty in the standard-siren  $H_0$  determination is approximately 10–15 per cent, but systematic convergence of many events will provide an independent arbiter of the  $H_0$  tension between local-ladder (SHOES) and early-universe (Planck CMB) determinations. This programme represents one of the most promising near-term cosmological applications of gravitational-wave astronomy.

## 6. FUTURE DETECTORS

Planned third-generation ground-based detectors include the Einstein Telescope (Europe) and Cosmic Explorer (USA). The Einstein Telescope is a triangular 10 km underground interferometer with xylophone configuration low-frequency cryogenic interferometer paired with high-frequency high-power interferometer aiming for order-of-magnitude strain sensitivity improvement and extension of the detection band to 3 Hz.<sup>12</sup> Cosmic Explorer proposes 20–40 km L-shaped surface detectors, pushing further into high redshift and enabling detection of stellar-mass binaries throughout cosmic history. These third-generation instruments will detect on the order of  $10^5$  compact-binary mergers per year, effectively surveying the entire stellar-mass binary population to cosmological distances.

The space-based Laser Interferometer Space Antenna (LISA), scheduled for launch in the mid-2030s, will observe the  $10^{-4}$ – $10^{-1}$  Hz band dominated by massive black-hole mergers, extreme mass-ratio inspirals (EMRIs) of stellar-mass compact objects into supermassive black holes, and a galactic foreground of double white dwarfs.<sup>12</sup> LISA will detect the mergers of  $100$ – $10^6$  solar-mass black holes throughout cosmic history, probing the seeding and growth of supermassive black holes from the first stars through the present. EMRIs will test general relativity to exquisite precision by mapping the spacetime geometry of supermassive black holes through tens of thousands of orbital cycles.

Pulsar-timing arrays, exploiting the exquisite rotational stability of millisecond pulsars as galactic-scale natural clocks, detect gravitational waves in the nanohertz band ( $10^{-9}$ – $10^{-6}$  Hz). In 2023 the NANOGrav, EPTA, PPTA, and IPTA collaborations independently reported evidence of a stochastic gravitational-wave background consistent with the Hellings–Downs correlation signature of an isotropic background<sup>14</sup>. The signal is most plausibly attributed to the unresolved population of supermassive black-hole binary inspirals, though cosmological-origin backgrounds from cosmic strings or phase transitions remain in contention. The nanohertz detection opens the low-frequency gravitational-wave window, complementing the ground-based kilohertz window and the forthcoming millihertz LISA window.

## 7. DATA ANALYSIS AND INFERENCE CHALLENGES

Detection and parameter estimation of gravitational-wave signals rely on sophisticated Bayesian and frequentist methods that have evolved rapidly with the observational cadence. Template-based matched filtering remains the dominant detection technique for compact-binary coalescences; the search maximises the signal-to-noise ratio against noise-coloured templates, using template banks covering the astrophysically plausible parameter space. Template-bank density is chosen to limit mismatch losses, typically to 3 per cent. Coherent network searches combine data from multiple detectors, improving significance and sky-localisation precision.

Unmodelled burst searches complement template-based methods, targeting signals from supernovae, cosmic strings, and other poorly modelled sources. Coherent WaveBurst, BayesWave, and oLIB pipelines run in parallel with template searches. Long-duration continuous-wave and stochastic-background searches require yet different algorithmic approaches tailored to persistent signals.

Parameter estimation employs Bayesian inference with stochastic sampling. Markov-chain Monte Carlo, nested sampling (dynesty, CPNest), and more recently machine-learning-accelerated samplers (normalising flows, conditional density estimators such as DINGO) have been deployed to reconstruct posteriors over 15–17 source parameters within minutes to hours. Low-latency parameter estimation informs electromagnetic follow-up decisions; offline high-accuracy analyses use the full waveform model library and careful noise characterisation. Systematic uncertainties in waveform models, calibration, and detector noise are propagated through injection studies and coherent framework verification.

## 8. CONCLUSION

Gravitational-wave astronomy has consolidated into a routine observational science within a decade of first detection. The scientific harvest populations of compact objects, strong-field tests of general relativity, multi-messenger astrophysics, and standard-siren cosmology extends across the traditional disciplinary boundaries of astrophysics, fundamental physics, and cosmology. Future detectors including the Einstein Telescope, Cosmic Explorer, and LISA will deepen this harvest by extending the accessible mass and redshift ranges and by opening the low-frequency space-based window.<sup>12,13</sup> Pulsar-timing arrays have opened the nanohertz window with the first evidence of a stochastic gravitational-wave background in 2023. Together, these complementary windows promise a new era of gravitational-wave observation spanning more than twelve decades in frequency, from  $10^{-9}$  Hz to  $10^4$  Hz, and accessing sources from supermassive black-hole binaries through to stellar-mass compact coalescences and the cosmological neutron-star background. The decade ahead will refine the compact-binary census, sharpen cosmological constraints, and probe fundamental-physics regimes inaccessible to any other observational technique.

## REFERENCES

1. Abbott BP, Abbott R, Abbott TD, et al.; LIGO Scientific Collaboration; Virgo Collaboration. 2016. Observation of gravitational waves from a binary black hole merger. *Physical Review Letters*. 116(6):061102.
2. Abbott BP, Abbott R, Abbott TD, et al. 2017. Multi-messenger observations of a binary neutron star merger. *Astrophysical Journal Letters*. 848(2):L12.
3. Einstein A. 1916. Näherungsweise Integration der Feldgleichungen der Gravitation. *Sitzungsberichte der Königlich Preussischen Akademie der Wissenschaften (Berlin)*. 688–696.
4. Weisberg JM, Taylor JH. 2005. The relativistic binary pulsar B1913+16: thirty years of observations and analysis. In: *Binary Radio Pulsars*. ASP Conf Ser. 328:25–31.
5. Buonanno A, Sathyaprakash BS. 2015. Sources of gravitational waves: theory and observations. In: *General Relativity and Gravitation: A Centennial Perspective*. Cambridge: Cambridge University Press. p. 287–346.
6. Aasi J, Abbott BP, Abbott R, et al. 2015. Advanced LIGO. *Classical and Quantum Gravity*. 32(7):074001.
7. Tse M, Yu H, Kijbunchoo N, et al. 2019. Quantum-enhanced Advanced LIGO detectors in the era of gravitational-wave astronomy. *Physical Review Letters*. 123(23):231107.
8. Abbott R, Abbott TD, Acernese F, et al. 2023. GWTC-3: compact binary coalescences observed by LIGO and Virgo during the second part of the third observing run. *Physical Review X*. 13(4):041039.
9. Mandel I, Broekgaarden FS. 2022. Rates of compact object coalescences. *Living Reviews in Relativity*. 25(1):1.
10. Abbott BP, Abbott R, Abbott TD, et al. 2016. Tests of general relativity with GW150914. *Physical Review Letters*. 116(22):221101.
11. Abbott BP, Abbott R, Abbott TD, et al. 2017. A gravitational-wave standard siren measurement of the Hubble constant. *Nature*. 551(7678):85–88.
12. Maggiore M, Van Den Broeck C, Bartolo N, et al. 2020. Science case for the Einstein Telescope. *Journal of Cosmology and Astroparticle Physics*. 2020(3):050.
13. Amaro-Seoane P, Audley H, Babak S, et al. 2017. Laser Interferometer Space Antenna. arXiv:1702.00786.
14. Agazie G, Anumarlapudi A, Archibald AM, et al. 2023. The NANOGrav 15 yr data set: evidence for a gravitational-wave background. *Astrophysical Journal Letters*. 951(1):L8.